Human Molecular Genetics, 2000, Vol. 9, No. 17 2553–2562

New mutations in MID1 provide support for loss of function as the cause of X-linked Opitz syndrome

Timothy C. Cox[1,3,+], Lillian R. Allen[1], Liza L. Cox[1], Blair Hopwood[1], Bruce Goodwin[2], Eric Haan[3] and Graeme K. Suthers[3]

[1]Department of Molecular Biosciences and ARC Special Research Centre for the Molecular Genetics of Development, Adelaide University, North Terrace, Adelaide, South Australia, Australia 5005, [2]Royal Children's Hospital, Herston, Queensland, Australia 4029 and [3]South Australian Clinical Genetics Service, Women's and Children's Hospital, North Adelaide, South Australia, Australia 5006

Received 28 June 2000; Revised and Accepted 18 August 2000 DDBJ/EMBL/GenBank accession nos AF269101, AF272851

Opitz syndrome (OS) is a genetically heterogeneous malformation disorder. Patients with OS may present with a variable array of malformations that are indicative of a disturbance of the primary midline developmental field. Mutations in the C-terminal half of MID1, an RBCC (RING, B-box and coiled-coil) protein, have recently been shown to underlie the X-linked form of OS. Here we show that the *MID1* gene spans at least 400 kb, almost twice the distance originally reported and has a minimum of six mRNA isoforms as a result of the alternative use of 5′ untranslated exons. In addition, our detailed mutational analysis of *MID1* in a cohort of 15 patients with OS has resulted in the identification of seven novel mutations, two of which disrupt the N-terminus of the protein. The most severe of these (E115X) is predicted to truncate the protein before the B-box motifs. In a separate patient, a missense change (L626P) was found that also represents the most C-terminal alteration reported to date. As noted with other C-terminal mutations, GFP fusion constructs demonstrated that the L626P mutant formed cytoplasmic clumps in contrast to the microtubular distribution seen with the wild-type sequence. Notably, however, both N-terminal mutants showed no evidence of cytoplasmic aggregation, inferring that this feature is not pathognomonic for X-linked OS. These new data and the finding of linkage to *MID1* in the absence of a demonstrable open reading frame mutation in a further family support the conclusion that X-linked OS results from loss of function of MID1.

INTRODUCTION

Opitz syndrome (OS) is a recent re-classification of two originally distinct clinical entities, Opitz G and Opitz BBB syndromes (1). The constellation of clinical manifestations defining OS include: (i) congenital heart defects such as atrial and ventricular septal defects, patent ductus arteriosus and coarctation of the aorta; (ii) a characteristic facial appearance (a broad nasal bridge, hypertelorism and low-set posteriorly rotated ears) with labiopalatine and laryngotracheal abnormalities; (iii) dysphagia and gastro-oesophageal reflux; (iv) abnormalities of the central nervous system (including major motor skill defects and developmental delay); and (v) genital anomalies e.g. hypospadias (2). Despite strict clinical criteria for initial diagnosis, retrospective investigations of families with affected individuals frequently reveal previously undiagnosed relatives who show isolated or mild clinical features (2). This clinical variability, even among males within the same family (2,3), has probably led to an underestimation of the true incidence of OS.

After two decades of uncertainty and debate about the underlying genetics of OS, evidence of genetic heterogeneity was provided by way of cytogenetic anomalies and linkage data for both autosomal (chromosomes 22, 13 and 5) and X-linked (Xp22) forms of the disorder (1,4–7). A gene, *MID1*, has recently been isolated from the Xp22 region and shown to harbour mutations in a number of patients with OS (8–10). *MID1* has been reported to encode a protein of 667 amino acids that contains an RBCC (RING finger motif, two B-box zinc finger motifs and a coiled-coil region) domain and a C-terminal domain of unknown function (8,11). Strikingly, most sequence changes in OS patients were noted to result in frameshifts although a few missense changes were described (8–10). All of these previously reported mutations resided within the C-terminal half of the protein (8–10), leading to the suggestion that some *MID1* function might be retained or a new function acquired (10,12).

Despite sharing similarity with a wide variety of nuclear factors including products of proto-oncogenes (e.g. PML, RFP) and proteins with developmental roles (e.g. *Pleurodeles waltls*, PwA33; *Xenopus laevis*, XNF7), recent studies have indicated that MID1 is a microtubule-associated protein (10,13). Consistent with an important developmental role, the murine *Mid1* gene (also called *Fxy*) is expressed nearly ubiquitously but most highly in the developing branchial arches consistent with the spectrum of craniofacial anomalies seen in patients with MID1 mutations (8).

[+]To whom correspondence should be addressed. Tel: + 61 8 8303 4812; Fax: +61 8 8303 4399; Email: timothy.cox@adelaide.edu.au

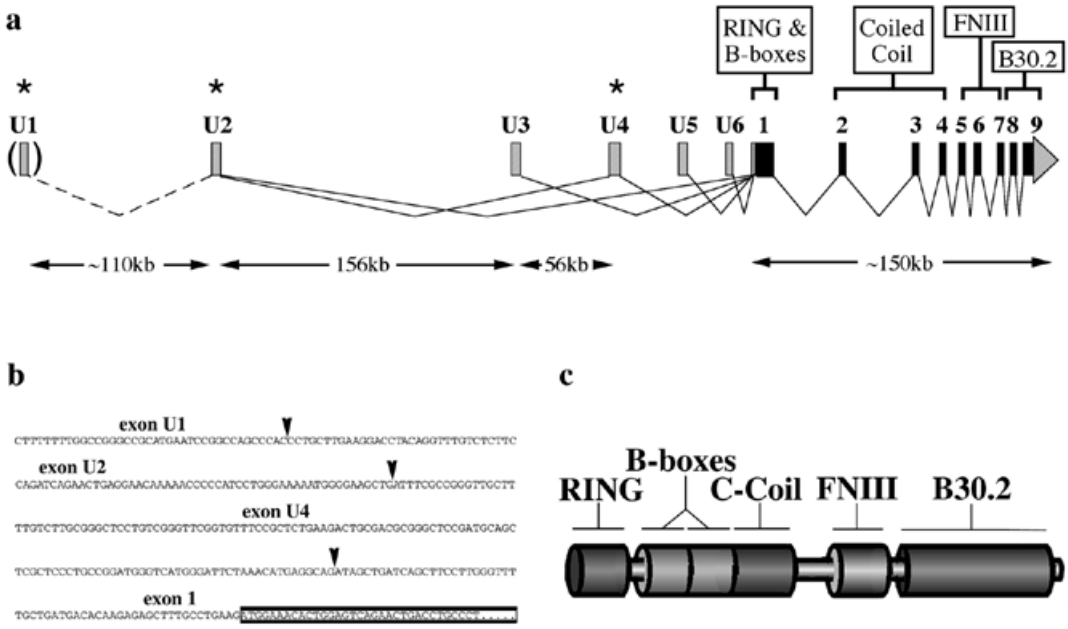

Figure 1. Structure of the *MID1* gene and protein. (**a**) Schematic representation of the exonic organization of the *MID1* gene showing approximate intron sizes. Black boxes, coding exons; hatched boxes, untranslated exons. The gene is transcribed in the centromere to telomere direction. Exons coding for the individual domains of the MID1 protein are indicated. Asterisked untranslated exons (U1, U2 and U4) were identified in our cDNA clones (GenBank accession no. AF269101). Exon U2 and the putative exon U1 have not been described previously, and only part of exon U4 had been reported. It is currently unknown whether exons U1 and U2 are utilized in all transcripts and therefore whether exons U3, U5 and U6 are alternatively utilized like exon U4. (**b**) Sequence and exon composition of the 5′ untranslated region of the largest *MID1* cDNA described in this report. Arrowheads indicate splice positions. The start of the coding sequence in exon 1 is boxed in black. (**c**) Structural representation of the MID1 protein shows the presence of a RING finger motif, two B-box motifs, a coiled-coil sequence and the C-terminal FNIII motif and B30.2 domain.

A total of 11 abnormalities in *MID1* have been published after screening >40 familial and sporadic cases (8–10). We now report a further seven unique mutations identified in our collection of 15 Australasian OS patients. Of particular interest were two mutations found in the N-terminal half of the protein that each affect the intracellular localization of the protein in a manner quite distinct from the C-terminal changes. Our findings not only significantly add to the spectrum of molecular defects that underlie the OS phenotype but also support the notion that the OS phenotype is caused by the loss of function of MID1, which is contrary to original proposals.

RESULTS

The *MID1* gene

Two large *MID1* cDNA clones have been isolated, the longest of which covers ~3.6 kb. Both sequences contained the complete open reading frame (ORF) of 2001 bp (8,11,12). However, our cDNA clones further extend the reported 5′ untranslated region by 92 bp and identify a further spliced sequence (Fig. 1a and b). The genomic organization of *MID1* was subsequently determined by fine restriction mapping and subsequent comparison of the cDNA to genomic sequence generated as part of the Human Genome Project. Our analysis showed that in addition to the nine coding exons that cover ~120–150 kb of genomic DNA (8,12) *MID1* possesses at least five 5′ untranslated exons that are differentially utilized (Fig. 1a and b). These sequences extend the gene size to ~400 kb, considerably larger than originally suspected. Moreover, a sixth untranslated exon (U1) may be represented by the first 38 bp of our cDNA sequence (Fig. 1a and b) although this region does not currently match any sequence in the genome databases. This may suggest that this 'exon' resides in the single remaining gap in the genomic sequence of this interval, which would position it ~110 kb further upstream of the U2 exon and increase the gene size to >500 kb. Alternatively, this short sequence may represent an artefact of cDNA library construction.

As previously shown, the *MID1* gene encodes a 667 amino acid protein with both an RBCC domain and a C-terminal B30.2 domain (8,11,12,14). Our recent finding of a region resembling the classic fibronectin type III repeat (FNIII) motif in the highly related factor MID2/FXY2 (14) prompted us to re-examine the reported MID1 domain structure (8–10,12). This detailed analysis using a variety of programs including PFAM, ProDom and Motif has shown that MID1 also possesses an FNIII motif (Fig. 1c) which exhibits 87.5% amino acid identity with the similarly positioned motif in MID2/FXY2 protein (14). This level of identity is higher than any other recognized domain within the two proteins. Furthermore, one OS patient (8) harbours a single amino acid deletion of a conserved residue (delM438) that resides within this predicted FNIII domain and this deletion disrupts the normal microtubular distribution of MID1 (10,13). These data support the likely

functional importance of this motif, the implications of which are further discussed below.

Clinical and cytogenetic findings in patients

In total, thirteen males and two females exhibiting features consistent with OS were included in the study. Because of the previous evidence for involvement of chromosome 22q11.2 as an autosomal OS locus (7,15–17), all patients, where possible, were tested for similar 22q11.2 anomalies by fluorescence *in situ* hybridization analysis. Of those 11 patients tested all were found to be negative for the common 22q11.2 deletion, although smaller submicroscopic deletions could not be ruled out.

A summary of the clinical and molecular findings in each case is presented in Table 1. In brief, eight of our fifteen patients presented with labiopalatine clefting whilst an additional two patients showed either just a highly arched palate or a bow-shaped upper lip. Ten patients presented with laryngo-tracheo-esophageal anomalies such as type I clefting. Four patients (OSP5, -6, -9 and -10) were noted as having one or more structural anomalies of the heart, including atrial and ventricular septal defects, coarctation of the aorta and patent ductus arteriosis (Table 1). An imperforate or anteriorly positioned anus was present in three patients. Ten patients had anteverted nares, one of two features suggested as possibly distinguishing the X-linked form of OS (2). Numerous patients exhibited additional features including two with limb and/or digit shortening and, interestingly, one with autistic features. Inferior cerebellar vermal agenesis (OSP9), a grooved tongue (OSP15) and eventration of the right diaphragm (OSP8), features not previously documented in OS, were also observed.

Mutations in isolated cases of OS

Eleven of the fifteen patients in this study were considered to represent isolated cases of OS as there was no evidence of a family history of the disorder. Nucleotide sequence alterations were identified in the *MID1* ORF of four (~36.4%) of these cases (Tables 1 and 2) and in at least one case (OSP12) where parental samples were available, the mutation was shown to have arisen *de novo* (Fig. 2b). For the remaining cases, the untranslated exons U2 and U4 were also tested for and shown to be present. For the description of all mutations in this report, nucleotide numbering was started from the adenosine residue (+1) of the ATG initiation codon. Mutation nomenclature was as per the recommendations of the Nomenclature Working Group (18).

Three of the four detected alterations were nonsense mutations: 1102C→T (R368X) in OSP3; 1483C→T (R495X) in OSP9; and 343G→T (E115X) in OSP12. The fourth change was a missense mutation, 1877T→C (L626P) in OSP5. Notably, of the mutations reported to date, E115X and L626P represent the N- and C-terminal-most changes. The E115X mutation truncates the MID1 protein at the first amino acid of the B-box motifs, whereas the R368X and R495X changes occur near the beginning of the FNIII repeat and C-terminal domain, respectively (Table 2).

To investigate whether the 1877T→C missense change identified in OSP5 was a polymorphism or a likely disease-causing alteration, single stranded conformation polymorphism (SSCP) analysis was performed on 50 control samples (Red

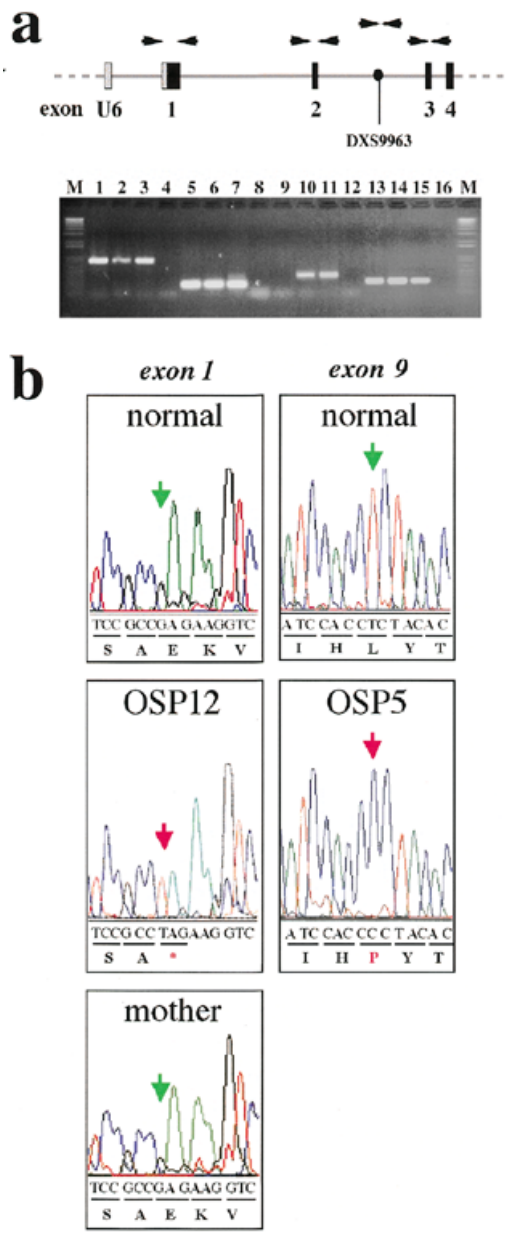

Figure 2. Mutational analysis of the *MID1* gene in patients with Opitz syndrome. (**a**) Demonstration that exon 2 is absent from OSP11. PCR amplification of exon 1 (lanes 1–4), exon 2 (lanes 9–12) and exon 3 (lanes 13–16) of the *MID1* gene and the sequence tagged site, DXS9963 (lanes 5–8). Lanes 1, 5, 9 and 13, proband (OSP11) samples; lanes 2, 6, 10 and 14, mother of proband; lanes 3, 7, 11 and 15, control human genomic DNA; lanes 4, 8, 12 and 16, no DNA control. M, *Eco*RI-digested SPP1 molecular weight markers. The relative positions of the exons and sequence tagged sites tested are indicated above the gel photo. Arrowheads represent primer locations. (**b**) Chromatograms of automated sequences from control (normal) and patient (OSP12 and OSP5) DNA. The altered nucleotides in the patient samples (343G→T in OSP12 and 1877T→C in OSP5) are indicated by the red arrows. The normal sequence is indicated by the green arrows. The exon location of each mutation is shown above the chromatograms. The subsequent changes in amino acid sequence (E115X in OSP12 and L626P in OSP5) are indicated by the red asterisk and red P, respectively. The corresponding chromatogram obtained from the mother of OSP12 is also indicated to show that the mutation in this individual has arisen *de novo*. The two mutations shown represent the N- and C-terminal-most alterations yet identified in patients with OS.

Table 1. Summary of the clinical features and molecular findings in the probands with Opitz syndrome involved in this study

	OSP no.														
Feature	1	2	3	4	5	6	7	8	9	10	11	12	13	14	15
Hypertelorism/telecanthus	Y	Y	Y	Y	Y	Y	Y	Y	Y	Y	Y	Y	Y	Y	Y
Prominent forehead	Y	N	Y	Y	Y	Y	Y	Y	Y	Y	Y	Y	N	Y	Y
Widow's peak	N	Y	Y	N	Y	Y	N	Y	Y	Y	Y	N	–	N	N
Broad nasal bridge	Y	Y	Y	Y	Y	Y	Y	Y	Y	Y	Y	Y	Y	Y	Y
Anteverted nares	Y	N	Y	Y	Y	n/a	Y	Y	Y	Y	Y	–	–	–	Y
Cleft lip/palate	N	Y	Y	Y	Y	Y	N	N	N	N	N	Y	Y	Y	N
High arched palate	–	n/a	Y	Y	N	n/a	N	Y	–	–	–	n/a	–	n/a	Y
Grooved nasal tip	N	N	N	N	Y	N	N	N	N	N	N	N	N	Y	N
Flat philtrum	Y	n/a	n/a	N	n/a	n/a	Y	Y	Y	Y	Y	n/a	–	n/a	N
Abnorm/post. rotated auricles	Y	N	Y	Y	Y	Y	N	Y	Y	Y	Y	Y	–	Y	Y
Laryngotracheal abnormality	Y	N	N	Y	N	N	Y	Y	Y	Y	Y	Y	N	Y	Y
Dysphagia/aspiration/GER	N	N	Y	Y	N	Y	Y	Y	Y	Y	Y	Y	Y	Y	Y
Congenital heart disease	N	N	N	N	Y (PDA; ASD)	Y (VSD; ASD CoA; +)	N	N	Y (VSD)	Y (VSD; PS)	N	N	N	–	N
Imperforate/anterior anus	N	N	N	Y	N	N	N	N	Y	N	N	Y	N	–	N
Hypospadias	Y	Y	Y	n/a	Y	Y	Y	Y	Y	N	Y	N	Y	n/a	N
Urinary tract abnormalities	–	N	–	N	N	Y	Y	N	Y	N	N	N	N	N	N
Cryptorchidism	N	N	N	n/a	N	N	N	N	N	N	N	N	N	N	N
Developmental delay	Y	Y	N	N	N	Y	Y	Y	Y	Y	Y	Y	N	Y	Y
Corpus callosum agenesis	N	N	N	N	N	N	–	–	N	N	N	N	N	N	N
Other features	COL	LDP		BPA		STR	DPH	MGN	IVA	HYC	AUT			LDS	INH
	DOD								LCM					CLN	UMH
	CAT								MSK					SYN	GRT
														MAL	MAC
															LDS
Sex	M	M	M	F	M	M	M	M	M	M	M	M	M	F	M
Family history	N	N	N	N	N	Y	N	Y	N	Y	Y	N (vWill)	N	N	N
22q11 region by FISH	Not deleted	–	Not deleted	Not deleted	Not deleted	Not deleted	Not deleted	–	Not deleted	–	–	Not deleted	Not deleted	Not deleted	Not deleted
MID1 nucleotide change	N	N	1102 C→T	N	1877 T→C	1051 delC	N	N	1483 C→T	1402 C→T	del Exon2	343 G→T	N	N	N
Protein change			R368X		L626P	Frame-shift			R495X	Q468X	del part CCoil	E115X			

Y, yes; N, no; –, not known; n/a, not applicable (e.g. features of philtrum after surgery for cleft lip); CAT, cortical atrophy; COL, coloboma of right macula; DOD, dysplastic optic discs; MGN, micrognathia; IVA, inferior vermal agenesis; LCM, large cisterna magna; HYC, hypoplastic cerebellum; BPA, Bell's palsy; MSK, mottled skin; LDP, multiple linear depigmented patches; vWill, von Willebrands; ASD, atrial septal defect; VSD, ventricular septal defect; PDA, patent ductus arteriosis; CoA, coarctation of the aorta; PS, pulmonary stenosis; +, other cardiac anomalies; LDS, limb/digit shortening; CLN, clinodactyly; SYN, syndactyly; INH, inguinal hernia; UMH, umbilical hernia; GRT, grooved tongue; DPH, diaphragmatic hernia; AUT, autistic features; MAC, macrocephaly; STR, strabismus; MAL, malrotation.

Cross Blood Bank, Adelaide, Australia). This missense alteration was not found in any of the control samples (data not shown) suggesting that it was not a common polymorphism. Furthermore, leucine[626] is completely conserved across all species (human, mouse, rat, chick and fugu) from which MID1 has been isolated (unpublished data). The amino acid is also

Table 2. MID1 mutations in X-linked Opitz syndrome

Nucleotide change	Amino acid change	Exon affected	Domain	Reference
343G→T	E115X	1	Before B-Box	This report
delExon2	Deletion of 1st third of coiled coil	2	Coiled coil	This report
796T→C	C266R	3	Coiled coil	9
948delG	Frameshift	4	Coiled coil	9
1051delC	Frameshift	5	Coiled coil	This report
1102C→T	R368X	5	Before FNIII	This report
IVS6-2A→G[a]	Skipping of final third of FNIII	7	Before FNIII	9
1312delATG	Deletion of M438	7	FNIII	8
1330insA	Frameshift	7	FNIII	13
1402C→T	Q468X	7	FNIII	This report
1483C→T	R495X	8	FNIII	This report
1483ins160bp	Frameshift	8	B30.2	9
1527ins13bp	Frameshift	8	B30.2	8
1558insG	Frameshift	8	B30.2	8
1601ins24bp	Insertion of 8 amino acids	8	B30.2	9
1607T→C	I536T	8	B30.2	9
1800delCCTC	Frameshift	9	B30.2	10
1877T→C	L626P	9	End B30.2	This report

[a]The predicted skipping of exon 7 (which encodes the final third of the FNIII motif) as a result of the putative splice-acceptor mutation (IVS6-2A→G) has not been confirmed experimentally.

conserved in the related MID2/FXY2 protein that overall shows ~76% identity with MID1 (14). Additional data from expression of the GFP–L626P fusion protein in cultured cells (see below) support the conclusion that this change does underlie the disorder in this individual.

A spectrum of mutations in familial cases of OS

Four familial cases of OS have also been examined, two of which had multiple affected individuals over four generations and were consistent with an X-linked mode of inheritance. Subsequent mutational analysis of affected individuals from all four pedigrees identified nucleotide alterations in three of the families (75%), including one frameshift (1051delC) in OSP6, one nonsense mutation [1402C→T (Q468X)] in OSP10 and a small deletion encompassing exon 2 (delExon2, OSP11) (Table 2; Fig. 2a). The exon 2 deletion is predicted to generate an in-frame deletion of 32 amino acids which represent the first third of the coiled-coil domain.

Of the familial cases, OSP8 was the only one in which we could not identify an underlying mutation in the *MID1* ORF. Furthermore, the untranslated exons U2 and U4 (Fig. 1a) were present and of the expected size in all affected male individuals of this family. Fortunately, this family was sufficiently large to justify haplotyping. This analysis was carried out using highly polymorphic microsatellite markers spanning three chromosomes only: the X chromosome and both chromosomes 22 and 13. These chromosomes were chosen as previous linkage studies (7) and cytogenetic abnormalities (5,6,15,17,19) had demonstrated that they were likely to harbour additional OS loci. Samples from the propositus, his mother and affected uncle, as well as his maternal grandmother and affected great uncle were available for analysis. These studies failed to show any shared chromosome 22 or chromosome 13 alleles. In contrast, three markers (DXS9994, DXS10006 and CxM40) from around the *MID1* gene in Xp22 demonstrated co-inheritance with the OS phenotype, indicating that the mode of inheritance in this large family is consistent with X-linkage and MID1 involvement (Fig. 3).

Consequence of OS mutations on MID1 intracellular localization

Transfection of constructs expressing the wild-type MID1 as a green fluorescent protein (GFP) fusion protein clearly showed colocalization of the protein with the microtubule network (Fig. 4a–d) as expected for endogenous MID1. However, expression of the C-terminal mutant forms of MID1 (R368X and L626P) as GFP fusion proteins revealed a punctate cytoplasmic distribution (Fig. 4m–t) that varied in appearance even between cells transfected with the same construct. In some cells numerous small fluorescent specks were visible throughout the cytoplasm, whereas in others few large perinuclear cytoplasmic clumps were present. These data appear consistent with the investigated C-terminal mutations reported by others (9,10,13). In contrast, the two mutations (E115X and delExon2) located in the N-terminal half of the protein showed strikingly different intracellular distributions. The delExon2 mutant protein (OSP11) was found diffusely distributed throughout the cytoplasm but excluded from the nucleus (Fig. 4i–l),

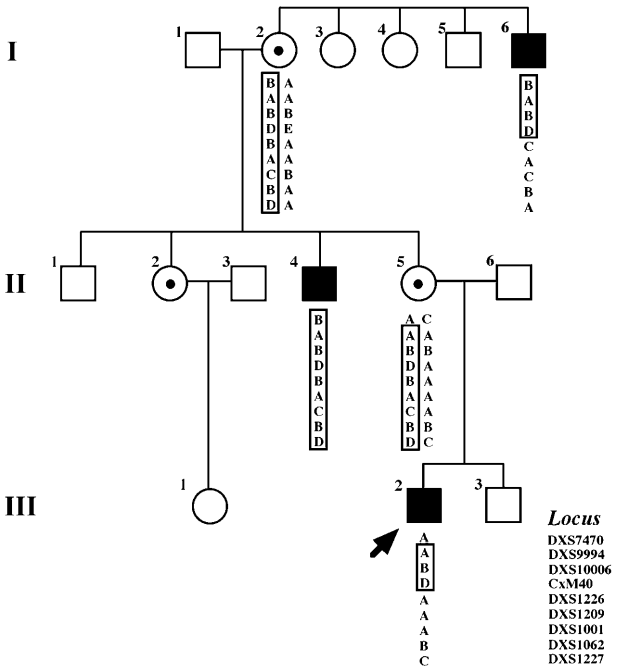

Figure 3. Haplotype analysis on the family of OSP8. Microsatellite markers spanning chromosomes X, 22 and 13 were typed on the available samples (individuals I.2, I.6, II.4, II.5 and III.2). The proband is indicated by the arrow. Only results of the X-linked markers are shown. Affected individuals are represented by black squares; open boxes and circles represent unaffected individuals. Individual I.6 presented with hypertelorism and cleft lip/palate and individual II.4 with hypertelorism, hypospadias and a laryngeal cleft. The mother and grandmother of OSP8 (individuals II.5 and I.2, respectively), are unaffected carriers and the maternal aunt (individual II.2) has hypertelorism, indicated by the small black dot within the circle. Marker alleles are represented by letters. The boxed alleles of individual I.2 were assumed to represent the ancestral chromosome. Boxed alleles in other individuals indicate those alleles in common with the 'ancestral' chromosome. All affected individuals (and carriers) share alleles for only DXS9994, DXS10006 and CxM40 (GenBank accession no. AF272851) which all reside in Xp22 around the *MID1* gene (21). No alleles of the tested markers from chromosomes 22 and 13 were shared among all affected individuals.

whereas the MID1 mutant truncated at amino acid position 115 (OSP12) and thus, encoding only the RING finger, was distributed throughout both the cytoplasm and nucleus (Fig. 4e–h). The nuclear GFP fluorescence of the latter mutant was particularly strong in comparison with the cytoplasmic signal. In both N-terminal mutants, there was limited overlay of GFP fluorescence and α tubulin staining in the cytoplasm. Whether or not this represented some residual interaction with the microtubules was not examined.

DISCUSSION

In order to gain a better understanding of the role of *MID1* in the pathogenesis of OS, we have performed a thorough mutational analysis of samples from 15 Australasian probands diagnosed with OS. In each case, all of the *MID1* coding exons have been screened for mutations using a direct sequencing protocol and any identified alterations examined for their effect on the subcellular distribution of the protein. In total, we have identified new and unique *MID1* gene alterations in seven (46.7%) of our patient cohort—four from our eleven isolated cases and in three of the four familial cases (Table 2).

Notably, an earlier and separate mutational screen performed on a collection of Opitz patients from the USA and Italy identified gene alterations in only 22.5% of their 40 cases (36% of familial cases and 6% of sporadic cases) (8,9). That underlying mutations in *MID1* could not be found in 77.5% of cases from this joint American/Italian study could be interpreted to suggest that the autosomal forms of OS are more common. Such a high proportion of autosomal-linked cases is, however, not consistent with our data or the low incidence of male-to-male transmission of OS in the literature. The discrepancy between the success rates in mutation detection may therefore reflect either the method employed for mutation screening (direct sequencing versus SSCP) or, alternatively, less stringent criteria for diagnosis. In this regard, many of our probands were identified because of their clinical severity, necessitating repeated surgical intervention. Unfortunately, comprehensive clinical descriptions for many of the individuals involved in the studies by Quaderi *et al.* (8) and Gaudenz *et al.* (9) have not been sufficiently detailed to allow any direct comparison with patients in our study. Although the overall percentage of mutations found in both studies is relatively low, an explanation may be found in the data generated from the only OS kindred in which we could not identify an alteration. In this familial case, haplotype data excluded the two autosomal loci investigated but clearly supported X-linked inheritance (consistent with *MID1* involvement). Our inability to detect this *MID1* mutation using a direct sequencing approach implies that the mutation in this family must lie outside the exon (and immediately flanking intron) sequences. A possible scenario is that the mutation in this family resides in a regulatory region of the gene ultimately leading to an altered level of MID1 protein. However, an intragenic rearrangement in this kindred cannot be excluded. On the other hand, if this case indeed harbours a *MID1* gene aberration, it would seem feasible that other similar cases (i.e. those without an identifiable *MID1* ORF mutation) would fall into this category of mutation and thus assist in realizing the true incidence of the X-linked form of OS.

As mentioned, all previously described *MID1* mutations in OS patients (11 in total) have been found in the C-terminal half of the protein (8–10,13). Eight (73%) of these changes were deletions or insertions, with the majority (75%) resulting in frameshifts and premature truncation of the protein. The remaining OS mutations were two missense alterations and a putative splice site mutation. In our study, mutations in the C-terminus of MID1 also predominated but mutations were not restricted to this region of the protein. Furthermore, of the C-terminal changes we have identified, only one was the result of an insertion or deletion. Instead, the majority of alterations in our cohort of patients were nonsense changes, with only a single mutation causing a missense (L626P) change. Interestingly, the latter affected a residue otherwise conserved between all MID1 and MID2/FXY2 proteins isolated to date.

Our finding that the MID1 protein also possesses an FNIII motif located between the tripartite RBCC and B30.2 domains prompted a re-analysis of the precise location of all reported mutations. Although disruption of the B30.2 domain has been purported as the major cause of the phenotype, our data now show that only eight of the eighteen mutations would affect

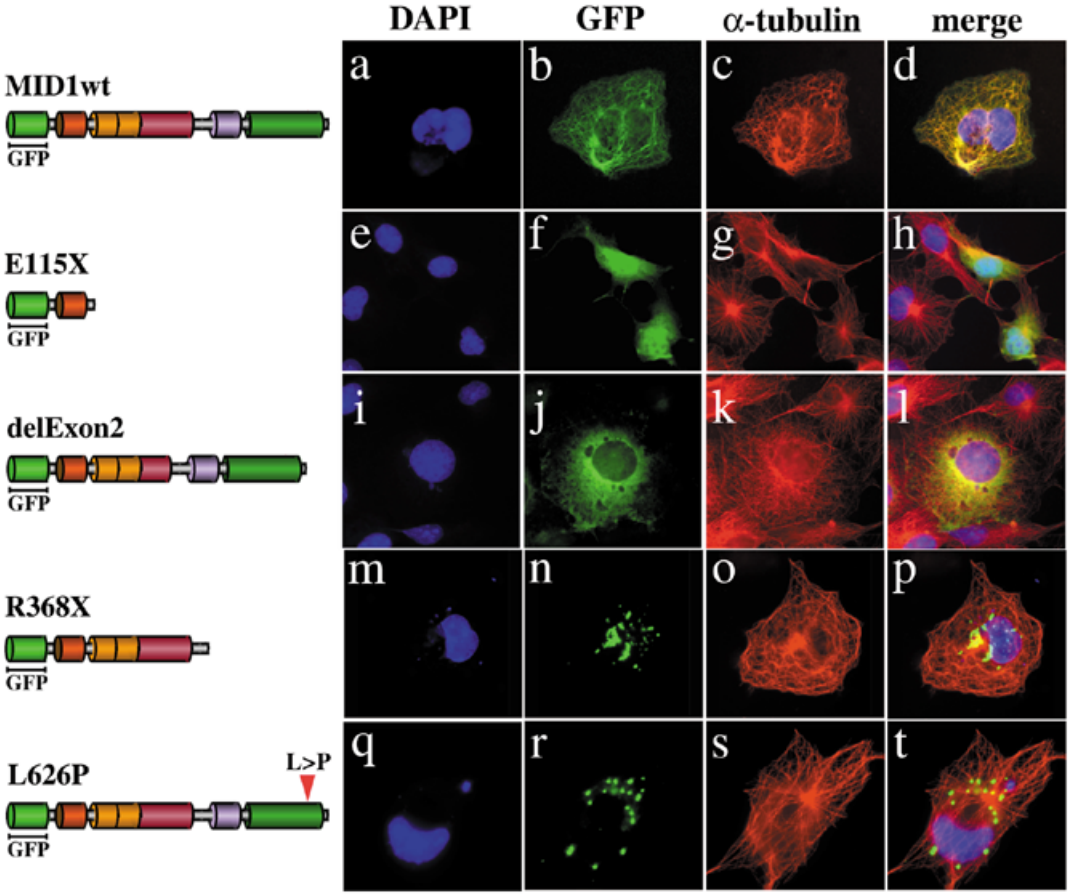

Figure 4. Transient expression of wild-type and mutant MID1 proteins in Cos1 cells. All MID1 proteins were expressed in Cos1 cells as GFP fusions, with the MID1 sequence fused to the C-terminal end of GFP. Wild-type GFP–MID1 (MID1wt) shows the expected colocalization with the microtubule network (**a**–**d**). The novel N-terminal mutant MID1–GFP fusion proteins, E115X (**e**–**h**) and delExon2 (**i**–**l**), do not colocalize with the microtubules. The E115X protein is found distributed throughout the cytoplasm and nucleus, whereas delExon2 is found only throughout the cytoplasm. The C-terminal mutants, R368X (**m**–**p**) and L626P (**q**–**t**) display a punctate distribution in the cytoplasm which is often perinuclear. Blue, DAPI nuclear stain; green, GFP fluorescence; red, anti-α tubulin. Colocalization is indicated by yellow coloration in merged images. These experiments were done in parallel and under identical conditions. All transfections have been repeated at least four times. The proteins expressed in each case are represented to the left. Expression of these constructs in HeLa cells gave essentially identical results (data not shown).

solely the B30.2 domain. Four additional mutations disrupt the FNIII motif and the B30.2 domain, with a further alteration (and possibly also the putative splice mutation) solely affecting the FNIII sequence. Of the remaining mutations, two affect just the coiled-coil motif, one the coiled-coil, FNIII and B30.2 motifs and our N-terminal mutation (E115X) which affects all but the RING finger motif (Table 2). Despite the diversity in nature and location of these mutations, there appears to be no obvious clinical difference between patients that would suggest any correlation between a patient's *MID1* genotype and the described phenotype. This is also supported by the clinical findings in familial cases of OS (for example, the large families of OSP6 and -8 in this study) where considerable variability in the severity of the OS phenotype is even found between males carrying the same X-linked mutation. Nevertheless, it is intriguing that all four patients with structural anomalies of the heart had demonstrable MID1 mutations.

In studies addressing the impact of C-terminal MID1 mutations, it was clear that all such aberrations abolish (or significantly reduce) the protein's association with the microtubule network (10,13). This disruption to the normal intracellular distribution of MID1 has been observed both *in vivo* in cells cultured from an aborted OS fetus (10) and following overexpression of the mutant protein in transfected cell lines (10,13). Interestingly, each of these MID1 mutants formed high molecular weight cytoplasmic complexes that did not have any obvious effect on the microtubule network. These observations led to the conclusion that disruption of the C-terminal (or B30.2) domain was the likely cause of the disease (10), despite a missense change having recently been found within the coiled-coil motif (13). This conclusion, however, is difficult to reconcile in light of our new findings (discussed below).

Using a similar transient transfection protocol for over-expression of MID1–GFP fusion proteins, we have investigated the effect of a number of our novel MID1 mutants on the protein's intracellular localization. Consistent with other MID1 C-terminal mutations (10,13) and analogous MID2/FXY2 C-terminal truncations (14), transfection of constructs expressing the L626P missense change or the R368X truncated MID1 protein revealed a punctate cytoplasmic distribution. Interestingly, the L626P mutation represents the C-terminal-most alteration

found to date yet, of the three reported missense changes, it appears to have the most significant effect on the intracellular distribution of MID1. This mutation highlights the likely importance of this B30.2 domain despite a specific function not yet having been ascribed to it.

With the previous observations that all OS mutations disrupt the normal microtubule association of MID1 and form cytoplasmic aggregates, we were curious to investigate the effect of our two novel N-terminal mutations on the intracellular localization of the protein. Transfection of constructs expressing each of these two mutant proteins was performed in parallel with transfection of the C-terminal mutants. Intriguingly, neither the E115X truncated protein nor the delExon2 in-frame deletion mutant showed any evidence of cytoplasmic clumping. Instead, the delExon2 protein was distributed diffusely throughout the cytoplasm, whereas the E115X mutant was diffuse throughout both the cytoplasm and nucleus. These findings are consistent with our other results that show that the B box region (or part thereof) is required for cytoplasmic retention of MID1 (unpublished data). Furthermore, the observations point to variable consequences of N- and C-terminal mutations on MID1 localization and demonstrate that cytoplasmic clumping of mutant MID1 is not pathognomonic for OS.

In considering the diverse effects of *MID1* mutation and the lack of any correlation between genotype and phenotype, our new data would imply that the clinical features of OS result from a loss of function of MID1. This conclusion is contrary to original thought (9,10,12) but is supported by three further observations: (i) that features of OS have been noted in females with MLS (or MIDAS) syndrome, a male lethal disorder associated with large Xp22 deletions that span the *MID1* gene (19); (ii) that MID1 expression is abolished in an OS patient carrying an inversion of the X chromosome that interrupts *MID1* upstream of the ORF (8); and (iii) the possibility of a regulatory region mutation in OSP8 (this study). The variability in clinical phenotype in OS patients may therefore depend on the ability of other factors [such as other microtubule-associated proteins (MAPs)] to compensate for the function of MID1 as has been suggested for other MAPs. It may then follow that those cell types normally showing high levels of MID1 expression would perhaps be more likely to be affected, for example the cells of the developing midline which contribute to many of the organs and tissues whose development is disturbed in OS patients. In this regard, one candidate compensatory factor could be the recently cloned MID1 homologue, MID2/FXY2 (14,20), that is expressed in similar tissues of the embryo but at a lower level (20). Genetic polymorphism at such loci could conceivably explain such marked inter- and intra-familial variability of the OS phenotype. Elucidation of the role of MID1 and MID2/FXY2 as well as the identification of MID1-interacting factors and regulatory molecules will therefore be important in dissecting the complex genetics and pathogenesis of OS.

MATERIALS AND METHODS

Isolation and characterization of MID1 clones

Full-length cDNA clones representing *MID1* were isolated by screening a human 26 week fetal brain 5′ stretch library (Stratagene, La Jolla, CA). The entire sequence was determined by a combined end-sequencing and primer walking strategy. *MID1* sequence analysis and database searches were performed via the internet using BLAST (http://www.ncbi.nlm.nih.gov) and locally using DNAsis v2.0 (Hitachi Software Engineering, San Bruno, CA). The amino acid sequence of MID1 was also analysed using a variety of web-based programs including Pfam, ProDom and Blocks.

The exonic organization of *MID1* was determined using radiolabelled primers and small fragments of cDNA as probes on digested cosmid DNAs selected from a previously described contig of clones (21). Exon–intron boundary sequence was obtained by either direct sequencing of cosmid DNA (and appropriately derived restriction fragments) with exonic primers or by sequence alignments with data generously provided by Prof. A. Ashworth and Dr J. Perry (Institute for Cancer Research, London, UK). As data were made available, comparisons with sequence generated as part of the Human Genome Project were also performed.

OS patients

Blood samples were collected with informed consent from 15 probands presenting with a diagnosis of OS. Samples were also gathered from parents when available as well as from other affected and non-affected relatives in the four cases with a confirmed family history of OS (OSP6, -8, -10 and -11).

Mutation analysis

To screen the *MID1* gene for mutations, genomic DNA was first prepared from whole blood as previously described (22). Coding exons were then amplified and directly sequenced from each of the 15 patients. In order to achieve this, primers were designed flanking each coding exon with the exception of the final exon where two overlapping primer sets were used. All primer sequences are available on request to the corresponding author. Standard amplification and automated sequencing protocols using dye terminator or big dye chemistry were employed for each exon. Reaction products were analysed on Applied Biosystems 373 and 377 sequencing machines at the Institute of Medical and Veterinary Science Sequencing Facility, Adelaide. Identified nucleotide alterations were confirmed by sequencing the complementary strand. Sequence of the larger exon 2 fragment was verified in each case using additional internal primers. Sequence alterations in the probands of familial cases were also verified by either direct sequencing or SSCP analysis of samples from additional affected and unaffected family members and, where appropriate, on 50 control samples. PCR was also performed on select patients in order to detect the presence and size of two of the 5′ untranslated exons, U2 and U4, using flanking intronic primers, 5′-GATTCCGAGCTGGACAGAGC-3′ with 5′-TGTGGGGTTAGAGGCTGAGC-3′ and 5′-GACAGAGTGCGTGTAGCAA-3′ with 5′-TGCTAACCCAGCAAGCTCTC-3′, respectively (Fig. 1a and b).

Linkage studies in the family of OSP8

Highly polymorphic microsatellite markers spanning the X chromosome (DXS7470, DXS9994, DXS10006, CxM40, DXS1226, DXS1209, DXS1001, DXS1062 and DXS1227) and both chromosomes 22 (D22S264, D22S446, D22S1150,

D22S277, D22S423 and D22S1171) and 13 (D13S170, D13S280 and D13S285) were chosen for haplotyping of the OSP8 kindred, a large multi-generation family with numerous affected members. Each marker was amplified in the presence of [^{32}P]ATP and allele sizes determined following electrophoresis on 6% denaturing acrylamide gels and exposure to Hyperfilm (Amersham Pharmacia, Little Chalfont, UK) as previously described (23).

Generation of GFP–MID1 fusion constructs

MID1 was fused to the C-terminus of GFP using the following strategy: the entire *MID1* reading frame was enzymatically amplified using Pfu polymerase (Stratagene) with the primers 5′MID-fusion (5-GTGAATTCCTGAAGATGGAAACACTGGAGTC-3′) and G232-2 (5′-GTGAATTCGGGACACTTCTGGTGAG-3′) using the full-length *MID1* cDNA in pBluescript as template. The product was then digested with *Eco*RI and ligated into similarly restricted pEGFP-C2. The correct orientation and integrity of the insert was determined by restriction digestion and direct sequencing.

Constructs encoding the L626P missense mutation and the delExon2 mutant identified in OSP5 and -11, respectively, were created using the QuickChange Mutagenesis kit (Stratagene) with the following complementary primer pairs: P7128-F (5′-GAACTCCATCCACCCCTACACCTTCGACG-3′) plus P7128-R (5′-CGTCGAAGGTGTAGGGGTGGAGTTC-3′) and MIDOS12F (5′-GCAGCTTTGAGTGAGGTCAATGCATCACGT-3′) plus MIDOS12R (5′-CGTGATGCATTGACCTTCAATTTGTCATAGCG-3′), respectively. The truncated MID1 proteins resulting from the nonsense E115X (OSP12) and R368X (OSP3) mutations were also generated as GFP fusions. For the E115X mutation, the primers PE115Stop-R (5′-GTGAATTCTAGGCGGAGGTCATGGTG-3′) and EGFP-660 (5′-GATCACATGGTCCTGCTGGAG-3′) were employed in a PCR with Pfu polymerase and the GFP-MID wild-type clone as template. For the R368X mutation, the primers MID-CTD (5′-CTGCTCGAGCCCGCCTAGTTGATGGCCTTSACC-3′) and 5′MID-fusion were used with the full-length *MID1* cDNA in pBluescript as template. The resultant fragments were digested with *Eco*RI, and *Eco*RI plus *Xho*I, respectively, and cloned into similarly digested pEGFP-C2. All constructs were confirmed by restriction analysis and direct sequencing.

Transfection and image analysis of GFP–MID1 constructs

The various GFP–MID1 plasmid constructs were purified from 25–50 ml bacterial cultures using a Qiagen Midi kit (Qiagen, Hilden, Germany). Approximately 2 pmol of each construct were transfected into Cos1 and HeLa cells by electroporation or using FuGene transfection reagent (Roche Diagnostics Australia, Castle Hill, NSW). Cells were grown on a coverslip in Dulbecco's modified Eagle's medium supplemented with 10% fetal bovine serum, and 24 h post-transfection were fixed with 3.5% paraformaldehyde, 1× PEM buffer pH 7.0 (100 mM PIPES, 5 mM EGTA, 2 mM $MgCl_2$). Control microtubule staining was achieved post-fixation using an anti-α tubulin antibody plus a rhodamine-labelled secondary antibody (Roche Diagnostics Australia). Nuclei were stained using the DNA-specific stain, 4′,6-diamidine-2′ phenylindole dihydrochloride (DAPI; Sigma-Aldridge, Castle Hill, NSW). GFP and rhodamine fluorescence was visualized under appropriate wavelength light on an Olympus AX70 microscope (Olympus Australia, Mount Waverley, VIC). Images were captured using a Photometrics CE200A Camera Electronics Unit and processed using Photoshop 5.0 software (Adobe).

ACKNOWLEDGEMENTS

We would like to thank Professor Alan Ashworth and Dr Jo Perry for generously providing unpublished genomic sequence and information on the fugu *MID1* sequence, as well as Drs David Mowat, Nigel Clarke and Salim Aftimos for patients OSP13, 14 and 15, respectively. Thanks are also extended to Dr Christine Oley, Ms Erica Gurner and the National Heart Foundation of Australia Summer Scholars, Matthew Nicholls and Kirsten Farrand, for their valuable contributions. We are also grateful to the Department of Cytogenetics and Molecular Genetics, Women's and Children's Hospital, North Adelaide and the Cytogenetics Laboratory at the Royal Children's Hospital, Herston, for the chromosome 22q11 analyses. This work was supported by project grant no. 981165 and in part by both a C.J. Martin Fellowship and an R. Douglas Wright Award (no. 997706) (to T.C.C.) from the National Health and Medical Research Council of Australia.

REFERENCES

1. McKusick, V.A., Francomano, C. and Antonarakis, S.E. (1995) *Mendelian Inheritance in Man*, 11th edn. Johns Hopkins University Press, Baltimore, MD.
2. Robin, N.H., Opitz, J.M. and Muenke, M. (1996) Opitz G/BBB syndrome: clinical comparisons of families linked to Xp22 and 22q, and a review of the literature. *Am. J. Med. Genet.*, **62**, 305–317.
3. Opitz, J.M. (1987) G syndrome (hypertelorism with esophageal abnormality and hypospadias, or hypospadias-dysphagia, or Opitz-Frias or Opitz-G syndrome)—perspective in 1987 and bibliography. *Am. J. Med. Genet.*, **28**, 275–285.
4. Leichtman, L.G., Werner, A., Bass, W.T., Smith, D. and Brothman, A.R. (1991) Apparent Opitz BBBG syndrome with a partial duplication of 5p. *Am. J. Med. Genet.*, **40**, 173–176.
5. Verloes, A., David, A., Odent, S., Toutain, A., André, M.J., Lucas, J. and Le Marec, B. (1995) Opitz GBBB syndrome: chromosomal evidence of an X-linked form. *Am. J. Med. Genet.*, **59**, 123–128.
6. Urioste, M., Arroyo, I., Villa, A., Lorda-Sánchez, I., Barrio, R., López-Cuesta, M.J. and Rueda, J. (1995) Distal deletion of chromosome 13 in a child with the Opitz GBBB syndrome. *Am. J. Med. Genet.*, **59**, 114–122.
7. Robin, N.H., Feldman, G.J., Aronson, A.L., Mitchell, H.F., Weksberg, R., Leonard, C.O., Burton, B.K., Josephson, K.D., Laxová, R., Aleck, K.A. *et al.* (1995) Opitz syndrome is genetically heterogeneous, with one locus on Xp22, and a second locus on 22q11.2. *Nature Genet.*, **11**, 459–461.
8. Quaderi, N.A., Schweiger, S., Gaudenz, K., Franco, B., Rugarli, E.I., Berger, W., Feldman, G.J., Volta, M., Andolfi, G., Gilgenkrantz, S. *et al.* (1997) Opitz G/BBB syndrome, a defect of midline development, is due to mutations in a new RING finger gene on Xp22. *Nature Genet.*, **17**, 285–291.
9. Gaudenz, K., Roessler, E., Quaderi, N., Franco, B., Feldman, G., Gasser, D.L., Wittwer, B., Montini, E., Opitz, J.M., Ballabio, A. *et al.* (1998) Opitz G/BBB syndrome in Xp22: mutations in the *MID1* gene cluster in the carboxy-terminal domain. *Am. J. Hum. Genet.*, **63**, 703–710.
10. Schweiger, S., Foerster, J., Lehmann, T., Suckow, V., Muller, Y.A., Walter, G., Davies, T., Porter, H., van Bokhoven, H., Lunt, P.W. *et al.* (1999) The Opitz syndrome gene product, MID1, associates with microtubules. *Proc. Natl Acad. Sci. USA*, **96**, 2794–2799.
11. Perry, J., Feather, S., Smith, A., Palmer, S. and Ashworth, A. (1998) The human *FXY* gene is located within Xp22.3: implications for evolution of the mammalian X chromosome. *Hum. Mol. Genet.*, **7**, 299–305.
12. Van den Veyver, I.B., Cormier, T.A., Jurecic, V., Baldini, A. and Zoghbi, H.Y. (1998) Characterization and physical mapping in human and mouse of a novel RING finger gene in Xp22. *Genomics*, **51**, 251–261.

13. Cainarca, S., Messali, S., Ballabio, A. and Meroni, G. (1999) Functional characterization of the Opitz syndrome gene product (midin): evidence for homodimerization and association with microtubules throughout the cell cycle. *Hum. Mol. Genet.*, **8**, 1387–1396.
14. Perry, J., Short, K.M., Romer, J.T., Swift, S., Cox, T.C. and Ashworth, A. (1999) *FXY2*, a gene related to the X-linked Opitz syndrome gene *FXY/MID1*, maps to Xq22 and encodes a FNIII domain-containing protein which associates with microtubules. *Genomics*, **62**, 385–394.
15. McDonald-McGinn, D.M., Emanuel, B.S. and Zackai, E.H. (1996) Autosomal dominant Opitz GBBB syndrome due to a 22q11.2 deletion. *Am. J. Med. Genet.*, **64**, 525–526.
16. Fryburg, J.S., Lin, K.Y. and Golden, W.L. (1996) Chromosome 22q11.2 deletion in a boy with Opitz (G/BBB) syndrome. *Am. J. Med. Genet.*, **62**, 274–275.
17. Lacassie, Y. and Arriaza, M.I. (1996) Opitz GBBB syndrome and the 22q11.2 deletion. *Am. J. Med. Genet.*, **62**, 318.
18. Antonarakis, S.E. and Nomenclature Working Group (1998) Recommendations for a nomenclature system for human gene mutations. *Hum. Mutat.*, **11**, 1–3.
19. Kayserili, H., Cox, T.C., Cox, L.L., Basaran, S., Kylyc, G., Ballabio, A. and Yüksel-Apak, M. (2000) Molecular characterisation of a new case of Microphthalmia with Linear Skin defects (MLS): implications for the molecular and clinical classification of the syndrome. *J. Med. Genet.*, submitted.
20. Buchner, G., Montini, E., Andolfi, G., Quaderi, N., Cainarca, S., Messali, S., Bassi, M.T., Ballabio, A., Meroni, G. and Franco, B. (1999) *MID2*, a homologue of the Opitz syndrome gene *MID1*: similarities in subcellular localization and differences in expression during development. *Hum. Mol. Genet.*, **8**, 1397–1407.
21. Cox, T.C., Cox, L.L. and Ballabio, A. (1998) A very high density microsatellite map (1 STR/41 kb) of 1.7 Mb on Xp22 spanning the microphthalmia with linear skin defects (MLS) syndrome critical region. *Eur. J. Hum. Genet.*, **6**, 406–412.
22. John, S.W.M., Weitzner, G., Rozen, R. and Scriver, C.R. (1991) A rapid procedure for extracting genomic DNA from leukocytes. *Nucleic Acids Res.*, **19**, 408.
23. Cox, T.C., Kozman, H.M., Raskind, W.H., May, B.K. and Mulley, J.C. (1992) Identification of a highly polymorphic marker within intron 7 of the *ALAS2* gene and suggestion of at least two loci for X-linked sideroblastic anemia. *Hum. Mol. Genet.*, **1**, 639–641.